

# Correlation of Mean Velocity Measurements Downstream of a Swept Backward-Facing Step

Daniel J. Weber\*

*U.S. Army Chemical Research, Development and Engineering Center,  
Aberdeen Proving Ground, Maryland 21010*

and

James E. Danberg†

*U.S. Army Ballistic Research Laboratory, Aberdeen Proving Ground, Maryland 21005*

The effect of backward-facing step sweep angle on the mean turbulent velocity field has been measured at subsonic speeds. A single component hot-film anemometer was used in a wind tunnel to measure the velocity normal and parallel to three 1.27-cm-high, backward-facing steps with sweep angles of 0, 15, and 30 deg. A swept step flowfield provides a useful and special test case for modelers of three-dimensional turbulent flows. This is illustrated here by testing the ability of Coles' wall-wake model and the Baldwin-Lomax viscosity model's ability to describe the measured profiles. The Coles profiles are applied to regions of attached flow. The effects of sweep angle on the wake parameter  $\Pi$  downstream of reattachment is strong. The experimental outer-flow velocities were used to evaluate the constants in a modified form of the Baldwin-Lomax model. The resulting constants were in fair to good agreement with the recommended values except downstream of reattachment.

## Nomenclature

$A^+$	= Van Driest Damping Factor = 26
$a$	= constants used in fitting Coles' law
$C$	= intercept of the semilogarithmic law of the wall
$C_{cp}$	= Baldwin-Lomax constant = 1.6
$C_{wk}$	= Baldwin-Lomax constant = 0.25
$F_{max}$	= maximum moment of vorticity
$F(y)$	= moment of vorticity
$h$	= step height, 1.27 cm
$K$	= Clauser constant = 0.0168
$U$	= total velocity
$U_d$	= $u_{max} - u_{min}$
$U_e$	= total edge velocity
$U_\infty$	= freestream velocity
$u, v, w$	= velocity components along the $x', y', z'$ axes system, see Fig. 2
$u_e$	= $u$ -component edge velocity
$u^+$	= defined as $u/u_\tau$
$x, y, z$	= left-handed axis system aligned with wind tunnel, see Fig. 2
$x', y', z'$	= left-handed axis system aligned with step face, see Fig. 2
$y_{max}$	= distance above surface to maximum of the moment velocity
$y^+$	= defined as $yu_\tau/\nu$
$\Lambda$	= step sweep angle
$\Pi$	= Coles' wake parameter
$\alpha$	= total velocity flow direction angle
$\gamma$	= Klebanoff's intermittency factor
$\delta$	= boundary-layer thickness
$\delta_x^*$	= incompressible displacement thickness
$\kappa$	= von Kármán constant
$\mu_i^o$	= outer region eddy viscosity

$\nu$	= kinematic viscosity
$\rho$	= fluid density
$\tau$	= shear stress
$\omega$	= vorticity

## Introduction

AN extensive amount of information, both experimental and theoretical, is available on the flow over an unswept backward-facing step. For the swept backward-facing step the information available is limited to a phenomenological study performed by Selby,<sup>1</sup> a numerical analysis by Hartman et al.,<sup>2</sup> and mean velocity measurements made by Weber.<sup>3</sup> The flowfield over a swept backward-facing step is potentially of interest because it represents one of the simplest forms of a separated three dimensional flow. Although there are several reasons for this interest, possibly the most important is the role that this type of flowfield could play in the development and verification of three-dimensional turbulence models. The purpose of this study was to measure the effects of step sweep angle on the velocity field around a swept backward-facing step and then to correlate these results with Coles' composite law of the wall/law of the wake profile and the Baldwin-Lomax algebraic turbulence model.

## Description of the Flowfield

The flow over a swept backward-facing step is similar to the flow over a yawed cylinder as described by Schlichting.<sup>4</sup> The flowfield is an unique three-dimensional flow because it can be split into two separate flows. One flow is normal ( $u, v$ ) and the other is parallel ( $w$ ) to the step face. Theoretically, the normal flow is independent of the parallel flow. Thus, the equations representing ( $u, v$ ) and  $w$  velocity components can be decoupled which greatly simplifies the mathematical representation of the flowfield.

The different regions of the flowfield around a backward-facing step are illustrated in Fig. 1. Upstream of the step the flow exhibits typical turbulent boundary-layer development. At the step, the flow is forced to separate, thus creating a recirculation region. The recirculation region is separated from the remainder of the shear layer by a dividing streamline. As shown here the recirculation region is also divided by a stagnation line. It should be noted that this is a stagnation line in the  $x'-y'$  plane and a nonzero velocity component can exist

Received Sept. 17, 1991; presented as Paper 91-3240 at the AIAA 9th Applied Aerodynamics Conference, Baltimore, MD, Sept. 23-25, 1991; revision received May 5, 1992; accepted for publication May 7, 1992. This paper is declared a work of the U.S. Government and is not subject to copyright protection in the United States.

\*Aerospace Engineer, Aerodynamics Research and Concepts Assistance Branch, Member AIAA.

†Aerospace Engineer, Computational Aerodynamics Branch, Associate Fellow AIAA.

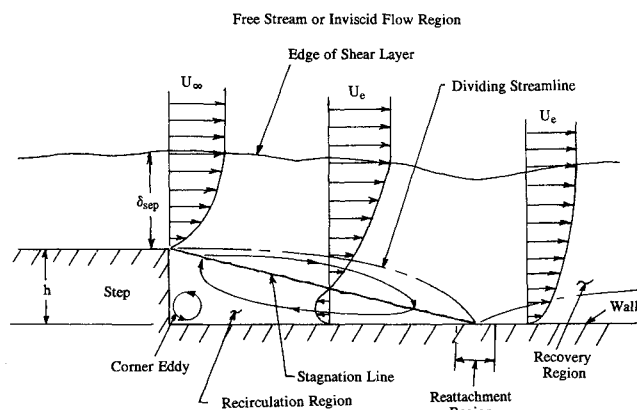


Fig. 1 Description of flowfield over swept backward-facing step.

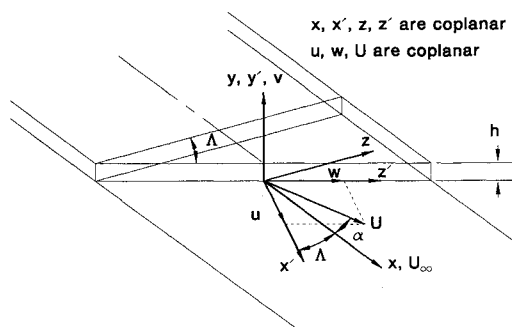


Fig. 2 Swept backward-facing step coordinate systems.

parallel to the step face. Downstream of the recirculation region is the reattachment region. It is here that the boundary layer redevelops as an attached turbulent boundary layer.

Figure 2 presents the coordinate systems used to describe the flow over a swept backward-facing step. The  $x, y, z$  coordinate system is aligned with the freestream flow direction in the wind tunnel, with  $x$  pointing downstream,  $y$  is vertical, and  $z$  horizontal. The  $x', y', z'$  coordinate system is aligned with the step face, with  $x'$  and  $z'$  being perpendicular and parallel to the step face, respectively, and  $y'$  in the same direction as  $y$ .  $U$  is measured with respect to the freestream direction by the flow angle  $\alpha$ .

## Experimental Study

### Wind Tunnel and Model

The experimental data in this study were obtained from tests conducted in a 0.7-m-high by 1.0-m-wide continuous flow subsonic wind tunnel at the Chemical Research Development and Engineering Center (CRDEC), Aberdeen Proving Ground (APG), MD. Velocity range of this tunnel is approximately 3 m/s to 70 m/s.

A flat-plate model was fabricated from 1.27-cm-thick Plexiglass® and spanned the entire test section. Three, interchangeable 1.27-cm-high steps, with sweep angles of 0, 15, and 30 deg, were attached to the flat plate. This step height, as well as the freestream velocity of 22.4 m/s, were chosen so that comparisons could be made with the study conducted by Selby.<sup>1</sup> All three steps had a centerline distance of 69 cm measured from the leading edge to the step edge. A grit strip was placed 5 cm downstream of the leading edge to assure transition to turbulent flow as far upstream of the step as possible. A sketch of the model relative to the test section is shown in Fig. 3.

Velocity measurements were made using a single-component hot-film anemometer which determined the local time-averaged velocity and flow angle in a plane parallel to the surface of the wind-tunnel model. The single-component probe was calibrated for both velocity and flow direction measurements.

A velocity calibration was performed with the probe perpendicular to the freestream flow. The wind-tunnel velocity was varied between 3 m/s to 33 m/s. Calibration for flow direction was accomplished by rotating the probe about its longitudinal axis from  $-60$  deg to  $+60$  deg in 10-deg steps with respect to the freestream. The reference position was 0 deg where the probe was perpendicular to the freestream. At each angle, the output of the probe was recorded, thus establishing the effect of flow direction on the probe's output. Probe positioning was accomplished using a height gauge, which allowed manual positioning of the hot-film probe to approximately  $25 \mu\text{m}$  above the surface of the wind tunnel model. The height gauge also allowed the probe to be manually positioned between 5.5 step heights upstream to 15 step heights downstream of the step. A description of the calibration and test procedure used in this study is presented by Weber and Danberg.<sup>5</sup>

With the probe calibrated, velocity profiles around the step were determined using the following technique. At a specific distance from the step, measured along the  $x$  axis, a series of velocity measurements were made at various heights above the model's surface. Each velocity measurement consisted of three readings, one with the probe rotated to  $-15$  deg, another at 0 deg, and the last at  $+15$  deg. From these three measurements, the magnitude of the total velocity and the flow direction in the  $x-z$  or  $x'-z'$  plane could be determined. The major disadvantage of using a single-component hot-film probe is that the probe could not resolve a flow reversal, as in the separated boundary layer. Detailed examination of the total velocity profiles produced evidence of flow reversal in some cases but this approach was only partially successful. Because of this limitation, the primary focus of the work was on the outer flow above the recirculation region.

Accuracy of the mean velocity flow direction and probe positioning above the model's surface is as follows. The uncertainty in measuring the total velocity is estimated to be within  $\pm 1$  m/s. The flow direction could be determined to within  $\pm 2$  deg for total velocities above 3 m/s and within  $\pm 10$  deg for velocities less than 3 m/s. Vertical probe positioning was within  $\pm 0.05$  mm.

## Experimental Results

Oil flow observations were made in order to determine the influence of the tunnel sidewalls on the flow over the model and also to compare the flow quality in this study with that obtained by Selby.<sup>1</sup> Overall the oil flow observations agreed well with Selby's results. No sidewall flow interference was detected within  $\pm 30$  cm of the model centerline.

Velocity profiles are presented as a series of carpet plots. The individual profile points are connected by straight lines and the zero position for each profile is indicated by a dotted line. Selected  $U$  profiles over the entire survey range for the 0-deg step are shown in Fig. 4. For the 0-deg step, the  $\alpha$  profiles were nearly zero; thus,  $U = u$  and  $w = 0$ . The profiles upstream of the step are typical turbulent boundary-layer

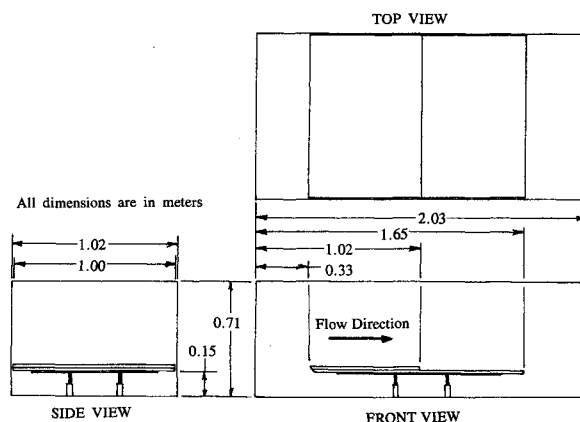


Fig. 3 Model installed in wind tunnel test section.

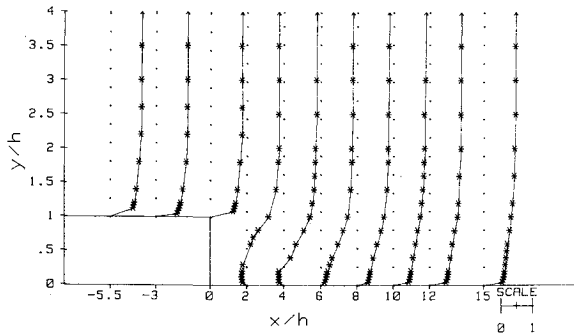


Fig. 4  $U/U_e$  profiles for  $\Lambda = 0$  deg and  $x/h = -5.5$  to  $15$ .

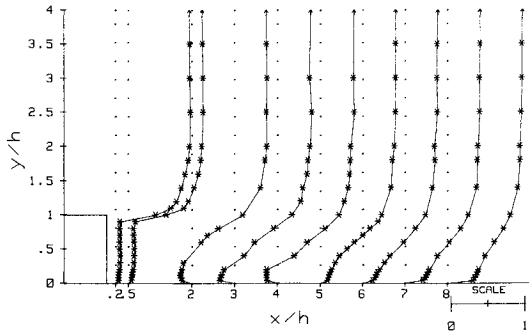


Fig. 5  $U/U_e$  profiles for  $\Lambda = 0$  deg and  $x/h = 0.2$  to  $8.0$ .

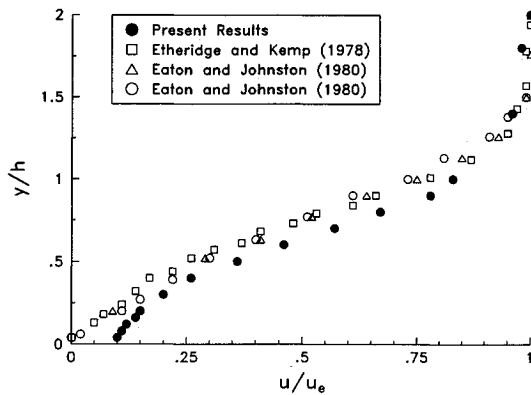


Fig. 6 Comparison of results ( $\Lambda = 0$  deg at and near reattachment).

profiles. The recirculation region can be seen between the step face and  $x/h = 5.0$ . From  $x/h = 6.0$  to  $15.0$ , a steady recovery of the flow from separation is indicated. Figure 5 shows the  $U$  velocity profiles  $x/h = 0.2$  to  $8.0$  in more detail. The results for the profiles at  $x/h = 0.2$  and  $0.5$ , below  $y/h = 1.0$ , are questionable because the measurements were outside of the calibration limits. Flow reattachment occurs between  $x/h = 4.0$  and  $5.0$ . Finally, downstream of reattachment, the flow continues to recover and the profiles become more full as  $x/h$  increases.

To check the measured data, a comparison was made with other investigators' unswept backward-facing step results. Results from the present study, Eaton and Johnston,<sup>6</sup> and Etheridge and Kemp<sup>7</sup> are presented in Fig. 6. Note that the Eaton and Johnston and Etheridge and Kemp profiles are at the reattachment point, and the present results are located approximately a half of a step height downstream. Taking this difference into account, the three profiles indicate good agreement.

The general trends for both the 15- and 30-deg configurations are very similar. Figures 7-10 show the 30-deg swept step carpet plots for  $U$ ,  $\alpha$ ,  $u$ , and  $w$ , respectively. The carpet plots for the 30-deg step, between  $x/h = 0.3$  to  $8.0$ , are presented as being typical results from this study. Similar to the unswept step, the portion of the profiles between  $x/h = 0.3$  to  $1.0$ ,

below  $y/h = 1.0$ , were outside of the calibration limits. The  $U$  profiles indicate a reattachment region between  $x/h = 3.0$  to  $4.0$  for the 30-deg step. Downstream of reattachment, the flow recovers with the profiles becoming more full as  $x/h$  increases. The  $\alpha$  profiles indicate that, in the recirculation region, the flow turns as it goes over the step so that it is flowing in a direction approximately normal to the step face. This flow pattern was also evident in the oil flow observations. Downstream of reattachment, the flow begins to realign itself with the freestream so that at  $x/h = 8.0$  the  $\alpha$  profiles are approximately zero. The  $u$  velocity component closely resembles the  $U$  profiles. The  $w$  component is positive in the recirculation and reattachment region near the model surface. This agrees

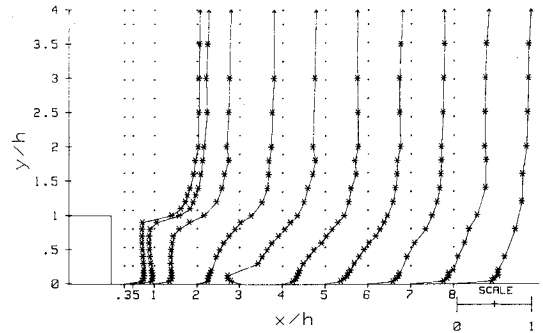


Fig. 7  $U/U_e$  profiles for  $\Lambda = 30$  deg and  $x/h = 0.3$  to  $8.0$ .

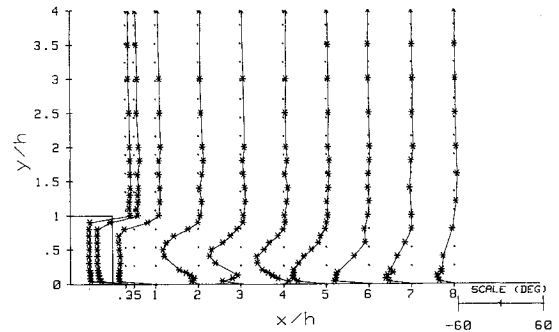


Fig. 8  $\alpha$  profiles for  $\Lambda = 30$  deg and  $x/h = 0.3$  to  $8.0$ .

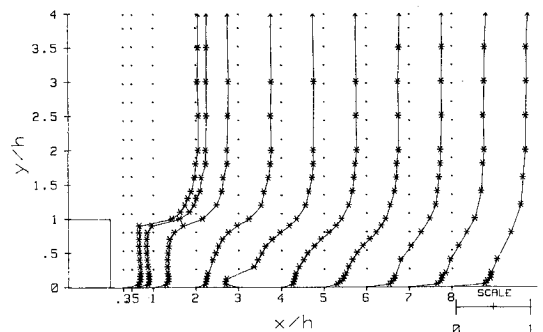


Fig. 9  $u/u_e$  profiles for  $\Lambda = 30$  deg and  $x/h = 0.3$  to  $8.0$ .

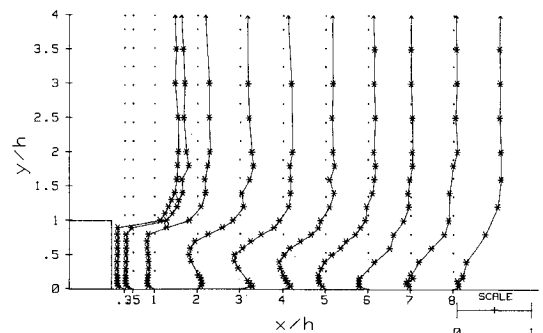


Fig. 10  $w/u_e$  profiles for  $\Lambda = 30$  deg and  $x/h = 0.3$  to  $8.0$ .

with the oil flow observations where the oil flowed parallel to the step in the recirculation region. Downstream of reattachment, the  $w$  velocity component is negative near the surface but slowly becomes positive as  $x/h$  increases.

**Correlation of Experimental Results**

Analysis of the results was accomplished in two parts. First, the experimental results corresponding to the attached profiles (those profiles upstream of the step and downstream of the reattachment region) were fitted to the Coles' composite law of the wall/law of the wake equation. The second part consisted of determining the Baldwin-Lomax constants for all profiles, both attached and separated.

**Coles' Composite Law of the Wall/Law of the Wake**

Coles' composite law of the wall/law of the wake can be useful in describing the velocity profiles in favorable and adverse pressure gradient turbulent boundary layers. Coles' profile as described by Cebeci and Smith<sup>8</sup> can be written as follows:

$$u^+ = \frac{1}{\kappa} \ln(y^+) + C + \frac{2\Pi}{\kappa} \sin^2\left(\frac{\pi y}{2\delta}\right) \tag{1}$$

where  $u^+ = u/u_\tau$ ,  $u_\tau = \sqrt{\tau/\rho}$  and  $y^+ = yu_\tau/\nu$ . This law is valid for the fully turbulent layer and across most of the outer region. The first two terms on the right-hand side of the equation represent the semilogarithmic form of the law of the wall.  $\kappa$ , the von Kármán constant, is the inverse of the slope and  $C$  is the intercept of the semilogarithmic law of the wall curve. The last term is Coles' wake function, which accounts for the wake defect of the velocity in the outer region of the boundary layer.

The constants in Eq. (1) are determined from the experimental results by a least-squares technique. This is accomplished by rewriting Coles' equation in the following form which was used by Danberg<sup>9</sup>:

$$u/u_e = a_1 \ln(y) + a_2 + a_3 \sin^2(a_4 y) \tag{2}$$

The  $a$  are four profile constants to be determined by the least-squares fit. A general, nonlinear least-squares fit routine was used to compute the four constants from four initial estimates by assuming small perturbations to the  $a$ . The procedure was repeated until a predetermined degree of accuracy was achieved. With the four values of  $a$  known, the constants,  $\Pi = a_3/2a_1$ ,  $\delta = \pi/2a_4$ , were determined without making any assumptions for  $\kappa$ .  $u_\tau/u_e$  and  $C$  can be obtained by choosing a value for  $\kappa$ . It is not possible to determine  $\kappa$  independently. Typical results for the wake parameter  $\Pi$  and the boundary-layer thickness  $\delta$  are presented in Figs. 11 and 12.

Figure 11 shows  $\Pi$  versus  $x'/h$  for the three sweep angles.  $\Pi$  is a function of the pressure gradient acting on the viscous flowfield. Coles and Hirst<sup>10</sup> evaluated a large number of incompressible turbulent boundary-layer profiles on flat plates at high Reynolds numbers ( $Re > 3000$ ) to obtain a value for  $\Pi$

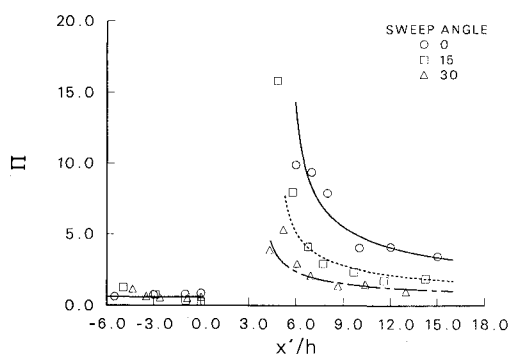


Fig. 11 Coles' wake parameter,  $\Pi$  vs  $x'/h$ .

of 0.55. Upstream of the step, an average value of 0.61 was obtained for  $\Pi$  (dropping two inconsistent values). Downstream of reattachment, the wake is the dominant component of the boundary layer. The inner or wall layer effectively disappears at reattachment and in the limit  $\Pi$  tends to infinity at reattachment. Then as the boundary layer redevelops downstream of reattachment the effects of the wall layer again become important. Although  $\Pi$  is slowly decreasing with downstream distance, it is still larger at  $x'/h = 15$  than its prestep value. The results also indicate that  $\Pi$  strongly decreases with increasing sweep angle.

The boundary-layer thickness  $\delta$  as determined from the least-squares fit of Coles' law and a power-law fit of the experimental results is presented in Fig. 12. Note that all boundary-layer thicknesses are shown with respect to the surface aft of the step. Both techniques are in good agreement. The general trend of  $\delta$  upstream of the step is to increase as the step is approached. The boundary-layer thickness at the edge of the step was estimated to be 2.24 step heights (referenced to the lower surface) using Schlichting's<sup>4</sup> turbulent boundary-layer relation. The agreement between experiment and theory is good to within 5%. In the recovery region  $\delta$  continues to grow with increasing  $x'/h$ . The effect of sweep angle  $\Lambda$  on  $\delta$  in the recovery region for a specific  $x'/h$  location shows that  $\delta$  increases with increasing  $\Lambda$ .

The resulting velocity profiles from Coles' equation, for  $\Lambda = 15$  deg, are shown in Figs. 13 and 14. Upstream of the 15-deg step all profiles collapse into a single curve which is illustrated in Fig. 13. Note that the solid lines represent Coles' velocity profiles and the symbols are experimental data. Downstream of reattachment, Fig. 14, Coles' profiles indicate flow recovery from separation and the profiles become more full as downstream distance increases.

**Baldwin-Lomax Algebraic Turbulence Model**

The Baldwin-Lomax model is a two-layer algebraic turbulence model used widely in computational fluid dynamics.

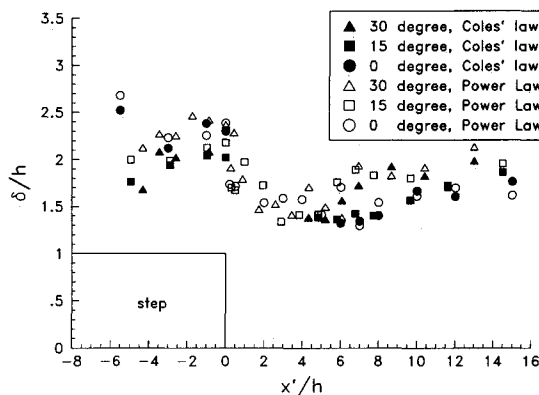


Fig. 12 Coles' and power law determination of  $\delta$ .

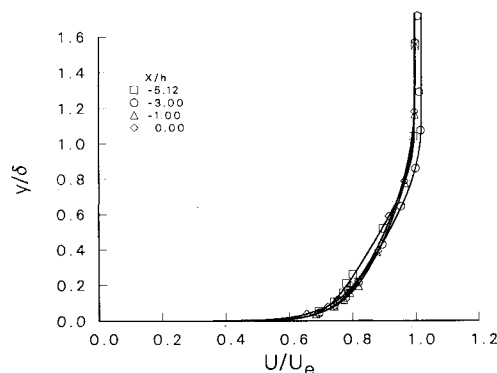


Fig. 13 Correlation of velocity profiles ahead of the step ( $\Lambda = 15$  deg).

Basically, the model evaluates the turbulent shear stresses in terms of an eddy viscosity with the major advantage that the boundary-layer thickness does not have to be known explicitly. The experimental results were considered more accurate above the reverse flow region and therefore the outer region Baldwin-Lomax formulation was used in correlating the velocity profiles. The outer region eddy viscosity model uses two different formulations, one for attached flows and one for separated flows. The attached flow outer region eddy viscosity is given by

$$\mu_t^o = KC_{cp}\rho y_{max}F_{max}\gamma \quad (3)$$

where  $K$  is the Clauser constant equal to 0.0168,  $C_{cp}$  is a constant equal to 1.6,  $\rho$  is the density, and  $y_{max}$  is the normal distance to  $F_{max}$  with  $F_{max}$  being the maximum moment of vorticity given by the following equation:

$$F(y) = y |\omega| [1 - \exp(-y^+ / A^+)] \quad (4)$$

where  $\omega$  is the vorticity and  $A^+$  is the Van Driest's constant. The last term in Eq. (3),  $\gamma$ , is Klebanoff's intermittency factor. The outer layer eddy viscosity for a separated flow is given by the following relation:

$$\mu_t^o = K\rho C_{cp}C_{wk}[U_d^2 y_{max}/F_{max}]\gamma \quad (5)$$

where the constant  $C_{wk} = 0.25$  and  $U_d$  is the difference between the maximum and minimum velocity across the profile. The model evaluates the value and location of the maximum moment of vorticity. A modification to Eq. (5) is necessary because the Baldwin-Lomax model does not properly account for the separation at a step, as discussed by Danberg and Patel. In going from the attached flow ahead of the step to the recirculation region, there is a discontinuous change in the magnitude and location of the maximum moment, unless the maximum vorticity in the shear layer is excluded. Thus, the basic Baldwin-Lomax model has been applied only above a displacement height corresponding to the first maximum of vorticity.

Because of the limited number of data points in the separated shear layer, a direct estimation of the vorticity was difficult. To avoid this problem, polynomials were fitted to the profiles in the separated region. The resulting polynomials adequately described the middle layer of the profile where the maximum moment of vorticity occurred. Using these polynomials, satisfactory results for  $y_{max}$  and  $F_{max}$  could be obtained, thus permitting determination of the Baldwin-Lomax constants.

An indirect procedure to determine the constants was used in which the Baldwin-Lomax viscosity formula was equated to the Clauser equation for eddy viscosity. The Clauser outer eddy-viscosity equation is based on empirical observations and has the following form:

$$\mu_t^o = K\rho\delta_k^* u_e \gamma \quad (6)$$

where  $\delta_k^*$  is the incompressible displacement thickness that can be evaluated from the experimental results. Equating Eq. (3) with Eq. (6) and Eq. (5) with Eq. (6) and then solving for the Baldwin-Lomax constants yields

$$C_{cp} = \delta_k^* u_e / F_{max} y_{max} \quad (7)$$

$$C_{cp}C_{wk} = \delta_k^* u_e F_{max} / U_d^2 y_{max} \quad (8)$$

This procedure provides a method of evaluating  $C_{cp}$  and the product  $C_{cp}C_{wk}$ . The values that these constants determined from the experiment were compared to those recommended by Baldwin and Lomax. The resulting constants are shown in Fig. 15. The average for the calculated  $C_{cp}$  upstream of the step is approximately 1.4 compared to a recommended value of 1.6.

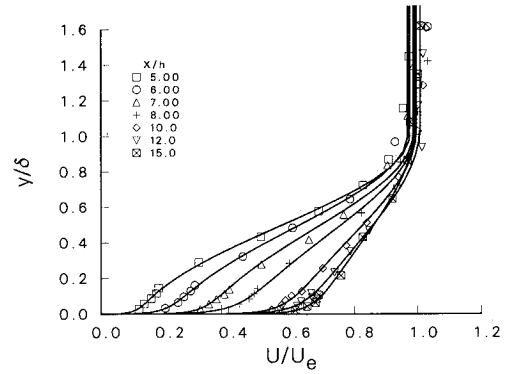


Fig. 14 Correlation of velocity profiles after reattachment ( $\Lambda = 15$  deg).

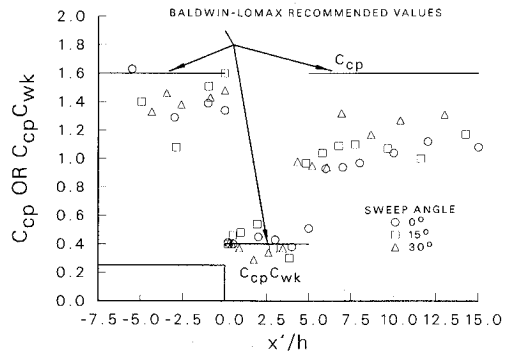


Fig. 15 Baldwin-Lomax constants for all profiles.

In the recirculation region, the average calculated  $C_{cp}C_{wk}$  is 0.4 which is the value Baldwin-Lomax recommended. Downstream of reattachment, the average value of  $C_{cp}$  is approximately 1.1 when the recommended value is 1.6. However, there is some suggestion, at least for the 0-deg sweep case, of a trend of  $C_{cp}$  increasing with downstream distance in the recovery region.

Summary

The first measurements have been made of the velocity field upstream and downstream of swept (15 deg and 30 deg) backward-facing steps. The 0-deg step results are consistent with other studies. The primary influence of step sweep angle  $\Lambda$  on the flowfield downstream of a swept backward-facing step is that the flow tends to recover more quickly with increasing step sweep angle.

Coles' composite law of the wall/wake profiles were successfully fitted to the measured attached flow profiles for the three swept step configurations. Coles' profiles upstream of the step collapse to a single curve and the profiles downstream of the reattachment region show the flow recovering from separation as downstream distance increases. The evaluation of the Baldwin-Lomax constants from the measured profiles showed fair to good agreement with their recommended values. Swept step flowfield data shows promise as a special test case for validating three-dimensional turbulence models.

References

<sup>1</sup>Selby, G. V., "Phenomenological Study of Subsonic Turbulent Flow Over a Swept Rearward-Facing Step," Ph.D. Dissertation, Univ. of Delaware, Dept. of Mechanical and Aerospace Engineering, Newark, DE, 1982.  
<sup>2</sup>Hartman, R. M., Seidel, B. S., and Danberg, J. E., "Computational Study of Turbulent Flow Over a Swept Backward-Facing Step," *Proceedings of the 6th International Conference on Numerical Methods of Laminar and Turbulent Flow*, edited by C. Taylor et al., Vol. 6, Pt. 1, Pineridge Press, Swansea, Wales, UK, 1989, pp. 411-421.

<sup>3</sup>Weber, D. J., "Hot Film Velocity Measurements Downstream of a Swept Backward-Facing Step," U.S. Army, Chemical Research, Development and Engineering Center, CRDEC-TR-221, Aberdeen Proving Ground, MD, Aug. 1990.

<sup>4</sup>Schlichting, H., *Boundary-Layer Theory*, 7th ed., McGraw Hill, New York, 1979, pp. 248-252.

<sup>5</sup>Weber, D. J., and Danberg, J. E., "Mean Velocity Measurements Downstream of a Swept Backward-Facing Step," *Proceedings of Southeastern Conference on Theoretical and Applied Mechanics (SECTAM)*, Vol. 25, Atlanta, GA, March 1990, pp. 412-417.

<sup>6</sup>Eaton, J. K., and Johnston, J. P., "Review of Research on Subsonic Turbulent Flow Reattachment," *AIAA Journal*, Vol. 19, No. 9, 1981, pp. 1093-1100.

<sup>7</sup>Etheridge, D. W., and Kemp, H. P., "Measurements of Turbulent Flow Downstream of a Rearward Facing Step," *Journal of Fluid Mechanics*, Vol. 86, Pt. 3, June 1978, pp. 545-566.

<sup>8</sup>Cebeci, T., and Smith, A. M. O., *Analysis of Turbulent Boundary Layers*, Academic, New York, 1974, pp. 122-128.

<sup>9</sup>Danberg, J. E., "A Re-Evaluation of Zero Pressure Gradient Compressible Turbulent Boundary-Layer Measurements," U.S. Army Ballistic Research Lab., BRL-MR-1642, Aberdeen Proving Ground, MD, April 1973.

<sup>10</sup>Coles, D. E., and Hirst, E. A., (eds.) "Compiled Data," *Proceedings of the Computation of Turbulent Boundary Layers 1968 AFOSR-IFP Stanford Conference*, Stanford Univ., Stanford, CA, Aug. 1968, p. 42.

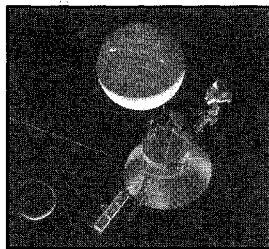
<sup>11</sup>Baldwin, B. S., and Lomax, H., "Thin Layer Approximation and Algebraic Model for Separated Turbulent Flows," AIAA Paper 78-257, Jan. 1978.

<sup>12</sup>Danberg, J. E., and Patel, N. R., "An Algebraic Turbulence Model for Flow Separation Caused by Forward or Backward Facing Steps," U.S. Army Ballistic Research Lab., BRL-MR-3791, Aberdeen Proving Ground, MD, Dec. 1989.

<sup>13</sup>Clauser, F. H., "The Turbulent Boundary Layer," *Advances in Applied Mechanics*, edited by H. L. Dryden and Th. von Kármán, Vol. 4, Academic, New York, 1956, pp. 1-51.

Offered in conjunction with the Aerospace Sciences Meeting and Exhibits, held at the Reno Hilton Resort, Reno, Nevada, January 11-14, 1993

#### Four Important AIAA Continuing Education Short Courses



■ **CFD on Parallel Processors**  
January 9 - 10, 1993 Reno, Nevada

■ **Theoretical and Computational Methods in Structural Acoustics**  
January 9 - 10, 1993 Reno, Nevada

■ **The Space Environment: Implications for Spacecraft Design**  
January 9 - 10, 1993 Reno, Nevada

■ **An Introduction to Interactive Computer Graphics**  
January 9 - 10, 1993 Reno, Nevada



American Institute of  
Aeronautics and Astronautics  
The Aerospace Center  
370 L'Enfant Promenade, SW  
Washington, DC 20024-2518

For additional information contact David Owens, Coordinator, Continuing Education  
TEL. 202/646-7447 FAX 202/646-7508